2003

Characterization of a Viscoplastic Constitutive Model and Its Application for the Finite Element Analyses of a Stirling Space Power Converter Heater Head

Ali Abdul-Aziz
Department of Civil & Environmental Engineering, National Aeronautics and Space Administration, Glenn Research Center, Cleveland, Ohio

David Krause
Life Prediction Branch, National Aeronautics and Space Administration, Glenn Research Center, Cleveland, Ohio

M. Tong
National Aeronautics and Space Administration, Glenn Research Center, Cleveland, Ohio

Taylor & Francis
Taylor & Francis Group

Characterization of a Viscoplastic Constitutive Model and Its Application for the Finite Element Analyses of a Stirling Space Power Converter Heater Head

ALI ABDUL-AZIZ

Department of Civil & Environmental Engineering,
National Aeronautics and Space Administration, Glenn Research Center,
Cleveland, Ohio

DAVID KRAUSE

Life Prediction Branch, National Aeronautics and Space Administration,
Glenn Research Center, Cleveland, Ohio

M. TONG

National Aeronautics and Space Administration, Glenn Research Center,
Cleveland, Ohio

ABSTRACT

NASA has identified the Stirling power converter as a prime candidate for the next generation power system for space applications requiring 60,000 hours of operation. To meet this long-term goal, several critical components of the power converter were analyzed using advanced structural assessment methods. Perhaps the most critical component, because of its geometric complexity and operating environment, was the power converter's heater head. Low-cycle fatigue and creep experiments on a nickel-base superalloy, Udimet 720 LI (low inclusions) and viscoplastic analyses for the Stirling starfish heater head were conducted. All testing was performed at temperatures of 625 to 820°C in air. This work was initiated to generate a unique and consistent database in support of a life prediction modeling effort aimed at characterizing Freed's viscoplastic model and verifying the key damage mechanisms. In general, this paper describes the life assessment of the heater head, which included the characterization of a viscoplastic material model, the thermal and structural analyses of the heater head, and the interpolation of fatigue and creep test results at several elevated temperatures for life prediction purposes.

INTRODUCTION

Today's spacecraft operate at relatively low power levels, supplied by state-of-the-art solar arrays and storage batteries. Tomorrow's power needs will increase significantly as
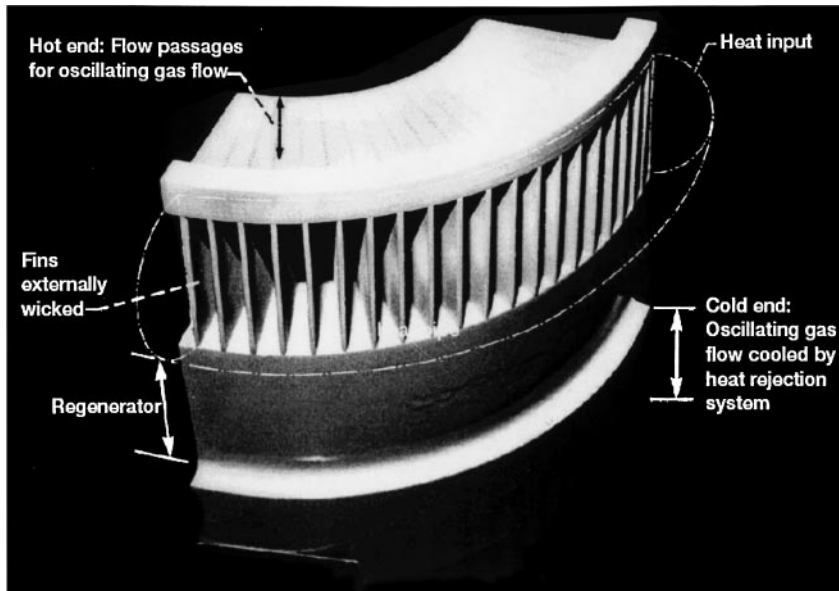
Figure 1. *Section of the "starfish" stirling engine heater head showing thin-walled fins.*

space-based missions evolve. Dynamic nuclear power systems utilizing the Stirling cycle show promise in meeting these needs.

Space power generating systems have stringent design requirements. They must be safe to launch and deploy, be reliable when called upon, exhibit a high efficiency-to-mass ratio, be economically feasible, and have long-term structural durability. Obvious trade-offs must be addressed among these requirements. In particular, low mass versus high durability trade-offs is of paramount concern for high-temperature, life-limiting components such as the heater head of a Stirling engine. The NASA Glenn Stirling Space Power Converter (SSPC) Project is using a geometrically complex heater head, referred to as the "starfish" heater head (Figure 1).

The SSPC project and the starfish heater head are discussed in references [1] to [3]. A cross-section of the Stirling Power Converter is shown in Figure 2. The heater head is a structural component that transfers heat from liquid sodium in the heat pipe to the working fluid (helium) of the power converter; it also includes the outer housing for the regenerator and cooler sections of the engine. The starfish heater is comprised of 50 fins, each containing 28 thin-walled gas passages. The fins are exposed to the liquid sodium at 775°C, which can attack the base metal of the starfish and degrade its durability. Further, the thin gas passage walls are under a biaxial stress state resulting from the high operating pressures $(15 \pm 1.8 \text{ MPa})$ of the converter [2].

The minimum life requirement for space Stirling power systems is 60,000 hours, with maximum operating temperatures in the range of 700 to 775°C [4]. At high operating temperature for extended periods of time, material response will invariably deviate from linear elastic behavior. Hot-section components of Stirling engines are subject to severe thermal gradients and high mechanical loads. Inelastic deformation will likely be induced in localized regions leading to eventual creep cracking and fatigue crack propagation. Udimet 720 LI, a cast-wrought nickel-base superalloy, is being considered for the starfish heater head material because of its long-term microstructural stability. It is a unique, nickel-base
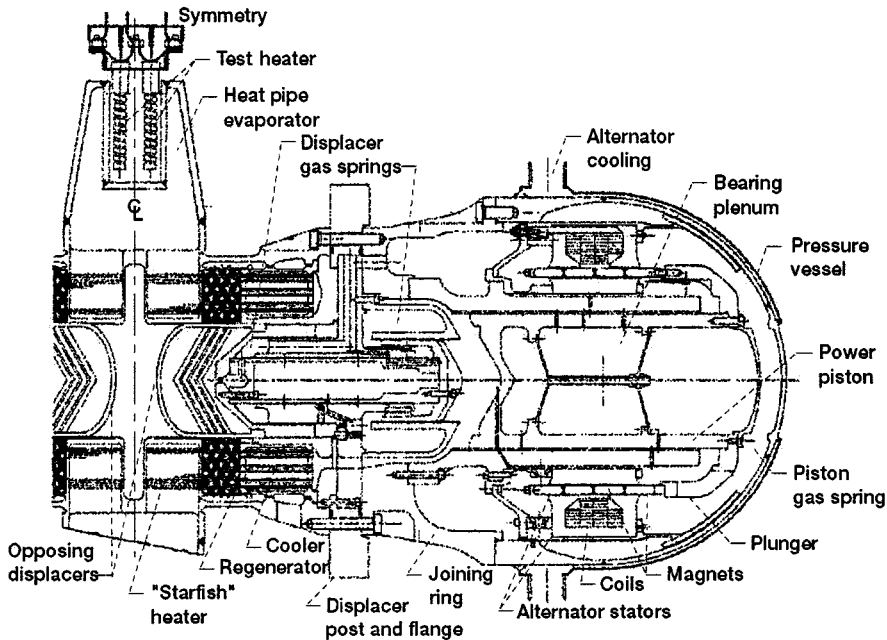
Figure 2. *Cross section of stirling power converter.*

gamma prime strengthened superalloy, which is used in elevated temperature applications requiring either high tensile strength with a fine-grain structure or high creep resistance with coarse-grain structure. In addition to its excellent strength, it has superior hot-corrosion resistance when compared to other wrought superalloys [5].

A final summary of a heater head life assessment conducted for the Stirling Space Power Converter Project at NASA Glenn Research Center is presented here. Included in this summary are Udimet 720 LI experimental stress-strain data collected through deformation, creep, and fatigue tests; this data was used for characterization of a viscoplastic constitutive model developed by Freed [6]. Also included is a description of the applicability of the material viscoplastic constitutive model and results of analyses conducted via the finite element method of the starfish heater head under thermo-mechanical loading conditions using the MARC code [7]. Lastly, a life assessment based on this information is presented.

It should be noted, however, that due to the lack of reliable stress-corrosion test data for Udimet 720 LI, this life assessment of the starfish heater head does not account for damage to the Udimet 720 LI resulting from direct contact with the liquid sodium. Thus, this life assessment represents the best-case condition, and any life reduction due to sodium caused corrosion is being compensated by an existing high margin of safety.

EXPERIMENTAL PROCEDURE

Material and specimens

Solid 0.31 mm diameter specimens of Udimet 720 LI were machined from a single heat of commercial grade Udimet 720 bar stock. The chemical composition of the alloy in weight percent is shown in Table 1 (internal report from Sczerzenie et al.: Udimet 720 Alloy. Special Metal Corp. Report TR-8-002, May 1978).

Table 1

Chemical composition of Udimet 720 (internal report from Sczerzenie, et al: Udimet 720 alloy. Special Metal Corp. report TR-8-002. May 1978)

Element	Weight percent
Carbon	0.01
Manganese	0.01
Silicon	0.01
Chromium	15.90
Nickel	Bal.
Cobalt	14.66
Iron	0.07
Monel	3.03
Tungsten	1.24
Titanium	5.08
Aluminum	2.70
Boron	0.0154
Zirconium	0.029
Sulfur	0.0011
Phosphate	0.001
Copper	0.03

Test apparatus and procedures

All the tests were performed on a 100-kN servo hydraulic axial test system. A personal computer was used for test control and data acquisition. Strains were measured using a commercially available axial extensometer. Two indentations were pressed into the outer surface of the specimen with a precision fixture so that the conical tips of the extensometer probes could be mounted. Specimen heating was accomplished using a 5-kW induction heating system coupled to a movable three-coil heating fixture [8]. This arrangement permitted the adjustment of the heat input distribution, thus allowing the thermal gradient within the gage section of each specimen to be kept to a minimum at any test temperature. Chromel-Alumel thermocouples, spot-welded just outside the gage section, were used to monitor and control the specimen temperature. Variation of the temperature along the uniform section of the specimen was within 1% of the nominal temperature. In each test, cyclic stress-strain data were acquired until failure of the specimen.

ANALYTICAL PROCEDURE

Freed's viscoplastic model

Prior to the computer revolution, viscoplasticity was a theory of its infancy; however, over the past two decades substantial advancements have been made in the theory [9]. Because of viscoplasticity's intrinsic nature, which leads to systems of first order, ordinary, differential equations that are nonlinear, coupled, and mathematically stiff, a unique mathematical structure (like elasticity) is not to be expected [10]. Nevertheless, these past two decades have given the viscoplastic community a vast wealth of experience with a variety of evolution equations that need to be verified and implemented through characterization

of models that have predictive capabilities that are in reasonable agreement with experiments [11]. Moreover, analytical studies of engine hot section components, such as turbine blades [12] and combustor liners [13], have demonstrated that classical methods do not always accurately predict the cyclic response of a structure, simply because of the lack of interaction between plasticity and creep. In addition to the inability to model the interaction between creep and plasticity, most of the classical plasticity theories suffer from an inability to model material behavior under cyclic loading conditions. Under such loading conditions, the classical theories are unable to predict the strain hardening/softening characteristics of the material. These limitations in constitutive modeling behavior had been discussed in some depth by Krempl [14].

In light of the above information, it is apparent that the best approach to improve the prediction of inelastic behavior of metals at high temperatures is the development of unified viscoplastic theories. These not only satisfy the experimental observation of the inseparability of creep and plastic strains, but also handle interaction and various deformation phenomena in a more natural manner.

The mathematical structure of the viscoplastic constitutive material model used here for the Stirling engine hot-section component structural assessment incorporated two state variables: the yield function and the back stress. The yield strength accounted for isotropic hardening effects, whereas the back stress accounted for kinematic hardening effects. These state variables were considered to evolve phenomenologically through competitive processes associated with strain hardening, strain-induced dynamic recovery, and time-induced thermal recovery. The model in its general form is written as follows [6]:

$$\dot{\sigma} = E(\dot{\varepsilon} - \dot{\varepsilon}_1 - \dot{\varepsilon}_T), \tag{1}$$

$$\dot{\varepsilon}_1 = \theta(T)f(\langle \|LS - B\| - Y \rangle), \tag{2}$$

$$\dot{B} = h_1\dot{\varepsilon}_1 - r_1 B\|\dot{\varepsilon}_1\|, \tag{3}$$

$$\dot{Y} = h_2\|\dot{\varepsilon}_1\| - r_2\theta(T), \tag{4}$$

where

$\dot{\sigma}$ = stress rate
E = modulus of elasticity
$\dot{\varepsilon}$ = total strain rate
$\dot{\varepsilon}_1$ = inelastic strain rate
$\dot{\varepsilon}_T$ = thermal strain rate
$\theta(T)$ = function of temperature
$f(X)$ = function of X
$\|X\| = (2/3)X_{ij}X_{ij}$
L = limiting state function
S = deviatoric stress tensor
B = back stress tensor
Y = yield function
h_1, h_2 = strain hardening functions
r_1, r_2 = recovery functions

Equation (1) assumes that the stress rate is proportional to the elastic strain rate. Equation (2) is the flow equation, which defines the inelastic rate as a function of applied stress, internal state variables, and temperature, whereas Eqs. (3) and (4) specify how the internal state variables evolve during deformation processes. The Macauley bracket
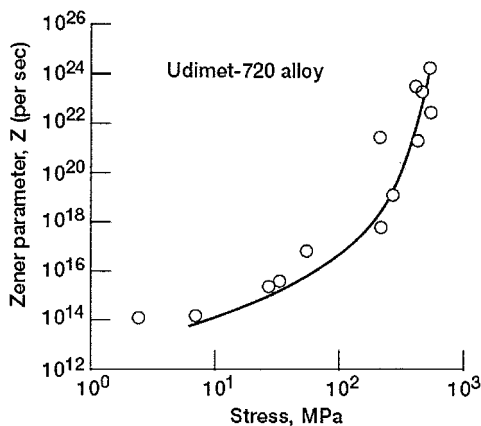
Figure 3. *Zener parameter as function of stress.*

operator $\langle \|S - B\| - Y \rangle$ has a value of 0 whenever $\|S - B\| < Y$ (defining the elastic domain), or a value of $\|S - B\| - Y$ whenever $\|S - B\| > Y$ (defining the viscoplastic domain), with $\|S - B\| = Y$ establishing the yield surface. The equations are chosen to reflect a particular metallurgical mechanism or phenomenological behavior.

To establish the temperature dependence of the viscoplastic model, the required material constants were determined using the experimental creep test data. The first step was the calculation of the steady-state Zener parameter [15], a temperature-normalized measure of the inelastic strain rate, utilizing the test data. The parameter was then plotted against its associated flow stress to obtain the curve, which characterized the steady-state creep behavior of the alloy (Figure 3). In the second step of the characterization process, the maximum values that can be attained by the stress and the internal variables were established via an estimation of the maximum Zener parameter. The final step included the partitioning of the internal stress between isotropic and kinematic contributions through the material constant *f*, and the quantification of the monotonic/cyclic interaction effects. Saturated, stress-strain hysteresis loops of the Udimet 720 were used during this process. The Levenberg-Marquardt minimization method was utilized to determine an optimal value for the material constant *f* (along with *D*). More details concerning the characterization process of Freed's viscoplastic model can be found in reference [6].

Other key requirements for the viscoplastic model were the material constants. These constants were determined through laboratory testing by performing the tensile, fatigue, and creep tests. The tests were conducted on smooth, uniaxial bar specimens fabricated from the same material and with the same heat treatment and composition specified for the component.

Finite element analysis

A three-dimensional finite element model (Figure 4) consisting of 5775 eight-node isoparametric brick elements and 8025 nodes was constructed using MSC/PATRAN Graphics [16]. Boundary conditions were applied to constrain all the nodes on the base to lie on a disk plane. Additional boundary conditions were imposed to prevent rigid body motion. Prior to conducting the analysis, a heat transfer analysis was performed to establish heater head temperature profiles. Thermal boundary conditions applied covered the convection
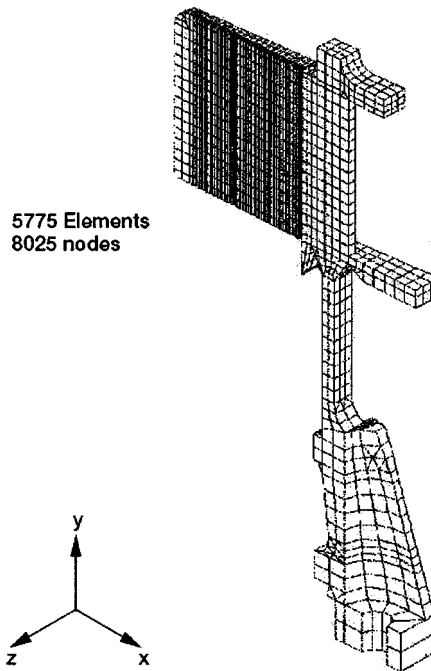
Figure 4. *Stirling heater head finite element model.*

between the air and the surrounding surface in addition to the conduction phenomena experienced by the material. Moreover, temperature dependency of all the material properties employed was accounted for in all the analyses. Convection trend inside the cooling passages was modeled by using a Nusselt number coefficient of 3.658 for laminar flow inside tubes [17]. Figure 5 shows the temperature distribution obtained from the heat transfer analysis. Note the large temperature gradient in the regenerator outer wall. In addition to the thermal load, a mechanical load based on gas pressure was included, and its severity is illustrated in Figure 6 in terms of load versus time. To minimize computational complexities, a 10,000 hours loading cycle was considered for the analysis.

Viscoplastic analysis

The viscoplastic model, developed by Freed [6], and characterized for Udimet 720 LI, was employed to describe the time-dependent inelastic behavior of the material. This viscoplastic model, in its general multiaxial form, was implemented in the finite element program MARC by Arya [18]. This was done through the MARC user subroutine HYPELA employing a self-adaptive time integration strategy [19] and based on the explicit Forward Euler method. It provided accurate and efficient integration of the constitutive equations. The implementation was first exercised on several uniaxial problems involving isothermal and nonisothermal loadings. The results obtained from the tests were compared with experimental data to validate the finite element implementation. Figure 7 represents a comparison of stress versus strain data for Udimet 720 at 675°C between the viscoplastic model and the experiment for a uniaxial case. Good agreement was achieved which indicated a successful implementation of the model. Later, the applicability of the model was tested via a stress analysis of the Stirling engine heater head.
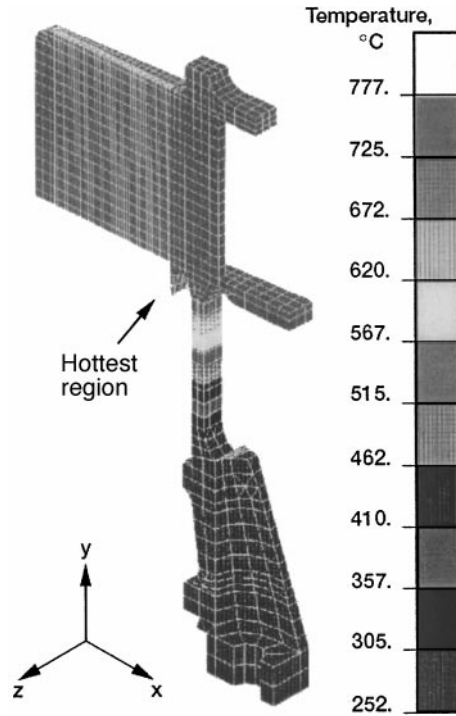
Figure 5. *Steady-state temperature distribution of heater head.*

RESULTS AND DISCUSSION

Experimental results for the Udimet 720 LI and an estimation of design life for the starfish heater head is presented in this section. Also a discussion of the Finite Element Analysis (FEA) used to confirm the prime contractor's analysis and estimate stress redistributions caused by Viscoplastic material behavior are included. It should be noted that the
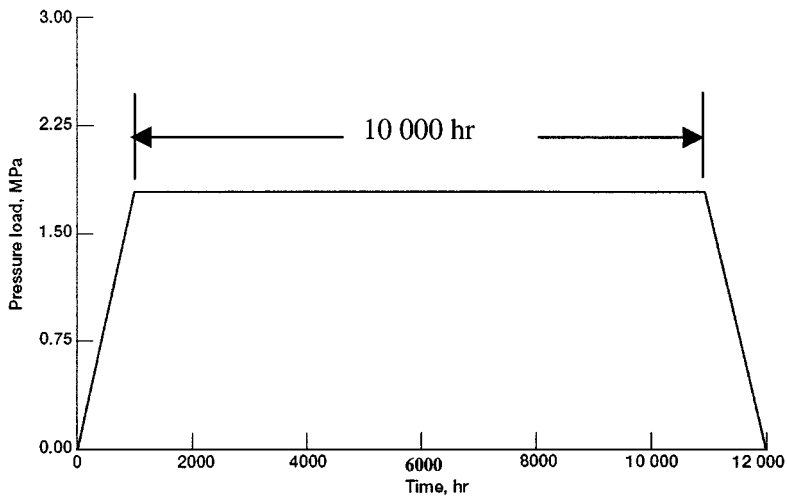

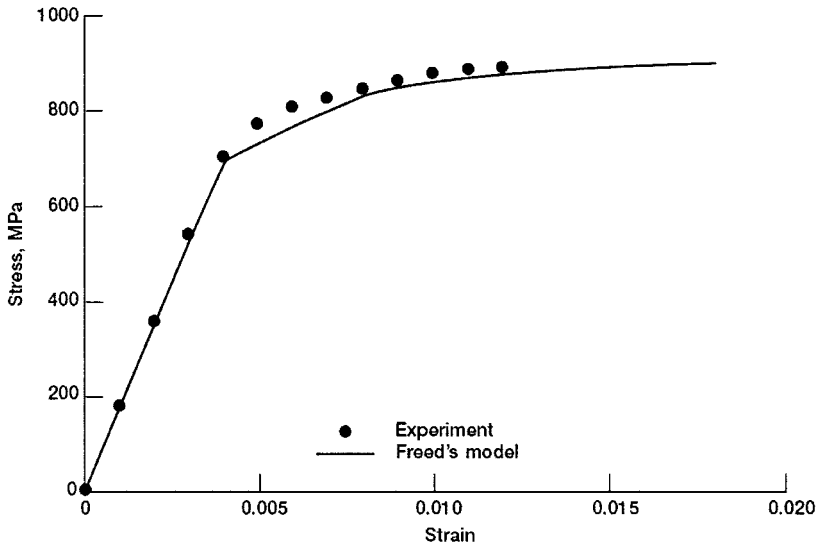**Figure 6.** *Loading cycle used for the analyses.*

Figure 7. *Stress-strain output for uniaxial test sample comparing experiment and prediction for Udimet 720 LI at 675°C.*

primary purpose of the database generated from this study was to characterize the constitutive model used for this FEA. Thus, test conditions and test termination points were chosen for this purpose and not to generate tensile, creep rupture, or fatigue data. Likewise, the life assessment was based on this data due to the limited existing Udimet 720 LI data for the design conditions.

Experimental test results

Tables 2 to 4 present tensile, creep, and fatigue data acquired from experiments conducted on Udimet 720 LI at the various noted test conditions. Tables 2 and 3 contain the tensile and creep results that were used in the model characterization and subsequent life assessment.

Table 2
Tensile data for Udimet 720

Specimen	Temperature °C	Strain rate, 1/sec	Modulus, Gpa	Stress, σ, at 0.1 percent, Mpa	Stress, σ, at 0.2 percent, Mpa
UD9	775	0.0001	172	744	771
UD8	775	0.0001	169	763	758
UD2	775	0.0003	171	775	802
UD5	775	0.0010	183	758	787
UD10	675	0.0010	189	822	853
UD11	820	0.0010	171	701	698
UD12	675	0.0010	184	785	816
UD13	625	0.0010	188	790	819
UD21	700	0.0010	186	821	853

Table 3
Steady state creep data for Udimet 720 LI

Specimen	Temperature °C (K)	Stress, σ, Mpa	Creep rate, 1/hr
CR1	820 (1095)	331	4.22×10^{-3}
CR2	820 (1095)	165	51.9×10^{-4}
CR3	775 (1050)	662*	1.15×10
CR4	775 (1050)	414	9.30×10^{-4}
CR5	775 (1050)	331	7.19×10^{-4}
CR6	675 (950)	827	7.86×10^{-2}
CR7	675 (950)	745	1.17×10^{-3}
CR8	675 (950)	662	5.19×10^{-5}
CR9	675 (950)	331	3.50×10^{-4}
CR10	675 (950)	331	1.94×10^{-5}
CR11	625 (900)	827	1.15×10^{-3}
CR12	625 (900)	745	7.35×10^{-4}
CR13	625 (900)	662	1.38×10^{-3}
CR14	625 (900)	414	6.69×10^{-5}

*Specimen ruptured after 4 hrs.

Tensile tests

The deformation response of Udimet 720 LI is presented in Figure 8. Note that test temperatures ranged from 625 to 820°C for all test types. These temperatures were chosen to create an envelope of material response around the proposed maximum operating temperature (775°C) of the starfish heater head. Due to instrumentation limitations, tensile tests
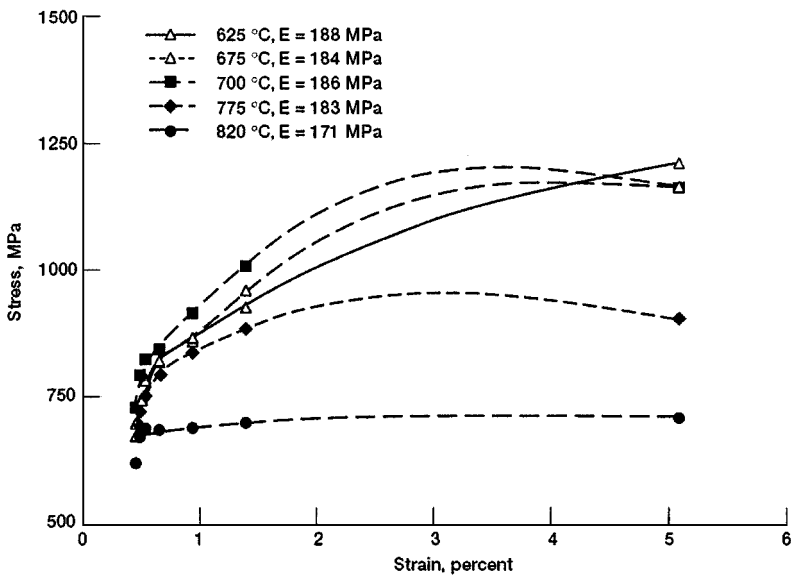

Figure 8. *Deformation response (stress-strain relation) for Udimet 720 LI.*

were stopped at 5% strain and were not taken to specimen fracture. Four of the tensile tests were used to investigate the strain rate sensitivity of Udimet 720 LI. Tests were conducted at 775°C with strain rates ranging from 10^{-4} to 10^{-3}/sec. Tensile results (Table 2) indicated that the Udimet 720 LI tensile properties were not significantly influenced by the strain rate. Therefore, a strain-loading rate of 10^{-3}/sec was used for subsequent tensile and deformation tests.

Creep tests

Likewise, for material model characterization purposes, creep stresses ranged between 165 and 827 MPa to encompass the desired stress-temperature combinations, (Figure 9). The tests were conducted at the various stress-temperature conditions to characterize the Zener parameter for the viscoplastic analysis (see earlier discussion) and to provide data for subsequent heater head life approximation. Tests were terminated after steady-state creep was achieved. Table 3 shows steady-state creep rates for all the tests at the different temperatures and stress conditions. The temperature ranged from 625 to 820°C. The stress level was varied from 165 to 827 MPa as the steady-state creep rate changed from a minimum of approximately 2×10^{-7}/hr to a maximum of approximately 1×10^{-2}/hr. One of the tested specimens at 662 MPa and 775°C ruptured after 4 hours.

Trends in steady-state creep rates with respect to stress and temperature are shown in Figure 9. The 675°C data had some scatter in creep rates, which is typical for creep data. It is noted that the variation of creep rate with respect to stress was similar at 675, 700, and at 775°C. The exception was the 820°C data, which was the maximum material test temperature. The slope for the 675°C temperature was steeper than for other temperatures. This provided a conservative (i.e., quicker) creep rate for a given applied stress lower than the test stress. Figure 10 shows the creep strain as a function of time for the entire temperature and stress range employed in the testing. Lower creep strain was reported at higher temperature and lower stresses.
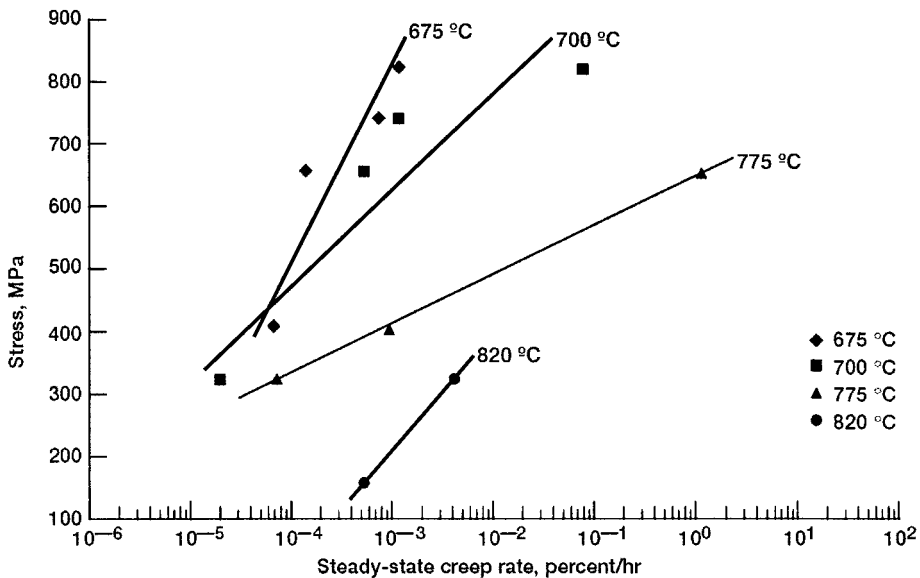

Figure 9. *Steady-state creep rate as function of temperature for Udimet 720 LI.*
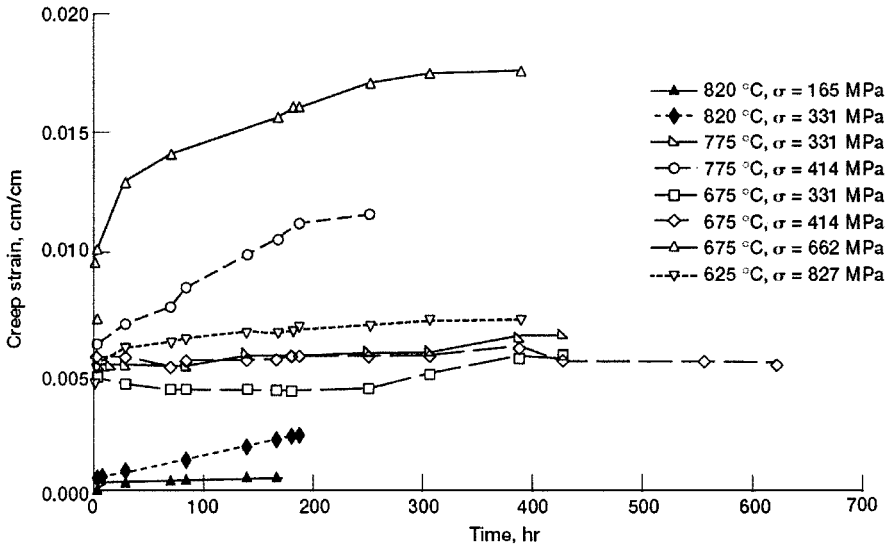
Figure 10. *Creep strain as function of time for Udimet 720 LI.*

Deformation tests

Results from a series of cyclic deformation tests are presented in Figure 11. These tests were conducted at a constant strain rate of 10^{-3}/sec and a constant strain range of 1.4%. The strain range was chosen from the heater head structural analysis (see later discussion). This analysis predicted that, for a start-stop-start sequence of the power converter, the heater head would experience, as a worst case, a maximum strain range of 1.4 percent.
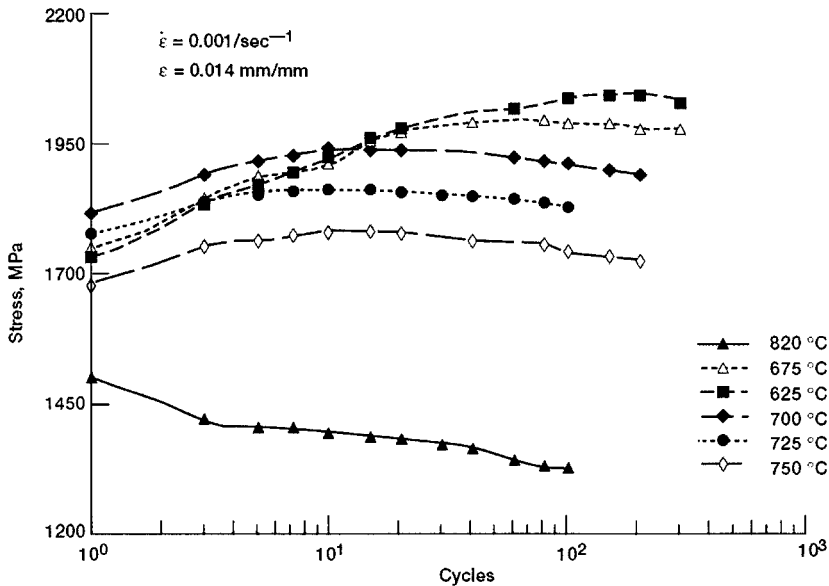

Figure 11. *Cyclic deformation for Udimet 720 LI.*

Table 4

Low cycle fatigue data for Udimet 720 LI on welded specimens (frequency, 02 Hz)

Specimen	Temperature °C	Strain. mm/mm	Life cycles
WU720-1	690	0.33	19,000
WU720-2	620	0.58	1,000
WU720-3	775	0.313	206,052

The hardening and softening characteristics of Udimet 720 LI are well observed in Figure 9. For example, at temperatures 675°C and below, the material exhibited hardening behavior. At the test temperatures of 750°C, Udimet 720 LI was cyclically neutral (i.e., the material neither hardened nor softened), and at 820°C, Udimet 720 LI appeared to exhibit softening characteristics. Since Udimet 720 LI was cyclically neutral at temperatures close to 775°C, all subsequent material modeling and structural analysis did not incorporate hardening/softening effects. This made the analysis less difficult and the computations less time intensive.

Fatigue tests

Fatigue data are presented in Table 4 for three different welded specimens, denoted by (WU), at three different temperatures. The fatigue life had a minimum of 1000 cycles and a maximum of 206,052 cycles. This showed that at the chosen combination of high temperature and low strain, the fatigue life was higher. All these specimens failed at the center of the test section as expected, and only three were available to test. Figure 11 shows the life cycle data generated from the testing, and it clearly indicates that the maximum life cycle never exceeded 1000 cycles for these particular-testing conditions.

Finite element results

The temperature profile illustrated in Figure 5 represents the temperature distribution as a result of a steady-state heat transfer analysis. It is clearly noticed that the top section of the heater head maintained a uniform temperature of about 777°C, whereas the temperature decreased as the helium fluid temperature changed from hot to cold as it moved from top to bottom. The lowest temperature experienced by the structure was 252°C located at the bottom portion, which was continuously cooled by the heat rejection system. A temperature gradient of about 500°C is apparent over the length of the outer wall of the regenerator.

Figures 12 to 15 represent the contours plots of the results predicted by the viscoplastic analyses at different times during the loading cycle. For example, Figures 12(*a*) and 12(*b*) represent the total mechanical stress and strain (Von Mises) distributions in the heater head after 1 hour's time. Figures 13(*a*) and 13(*b*) show similar results after 11,000 hours. The critical region, however, is noted to be in the starfish's thinned section of the heater head, as anticipated.

Thus, due to the combined effects of the temperature gradient and the mechanical loading, the outer wall of the regenerator exhibited the highest stresses and strains. Figures 14(*a*), 14(*b*), 15(*a*) and 15(*b*) represent the contours of the stresses and strains obtained predicted by Freed's model for the loading cycle of 1001 and 10,001 hours, respectively. These cases
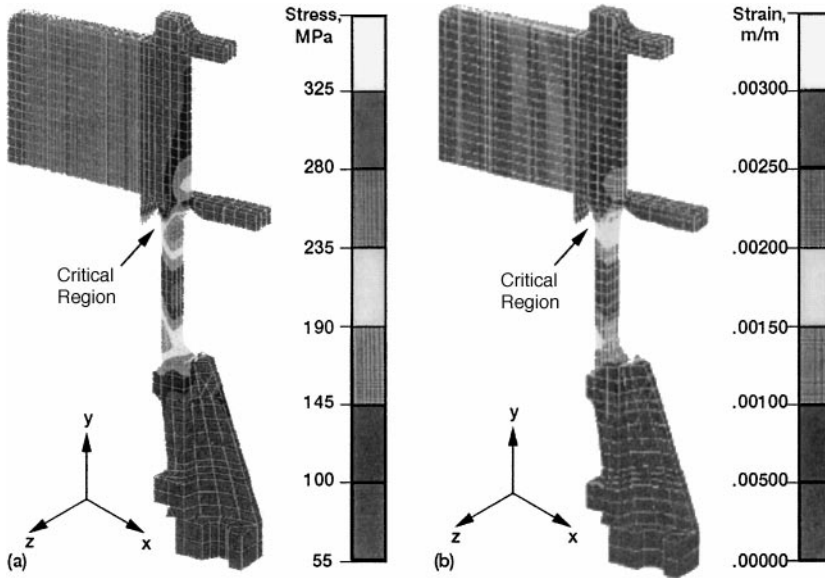
Figure 12. *Von Mises stress and equivalent mechanical strain predicted by Freed's viscoplastic model after 1 hour (*a*) Von Mises stress; (*b*) equivalent mechanical strain.*

were conducted in order to confirm experimental findings with respect to the operating life of the structure. In addition, it is demonstrated from these plots that the stresses relaxed and showed very minor change as time went from 1000 to 10,000 hours.

Life assessment

A preliminary life assessment analysis was conducted on the heater head. The assessment was based on lifing methodology from ASME code case N-47, the subject structural analysis, and the generated creep data from this study. Due to the limited resources and test data, the life assessment did not account for stress corrosion of the Udimet 720 LI caused by the liquid sodium. It is believed that due to many assumptions made during this assessment, a great degree of conservatism is warranted. And therefore, any degradation of life from the sodium would not drastically change the outcome of the approximation.

Results from the finite element analysis identified several critical locations in the heater head. These locations, along with their associated stress-temperature conditions, concurred with the designer's approximations. The two most critical locations in the heater head were located in the starfish's finned section; namely, (1) the leading tip of the fins and (2) the bottom of the fins in the gas passage area. At these locations, the temperature of the Udimet 720 LI was at a maximum of 775°C, and the calculated stresses were at a maximum of 235 and 140 MPa. The predominant failure mode for these areas was creep.

In addition to the relatively high temperature-stress condition in these areas, the Udimet 720 LI was subjected to corrosive liquid sodium. Liquid sodium can attack grain boundaries of alloys and has a high affinity toward nickel. Also, the gas passage wall thickness contributed to the criticality of this area. The combination of the starfish's thin wall and the requirement for a creep-resistant (large grain) Udimet 720 LI made it extremely vulnerable for failure. In the present design the grain size and gas passage wall thickness have been optimized to have an average of 3 to 5 grains spanning its thickness. Even though more grains going across that thickness is desirable from a structural integrity viewpoint, it will
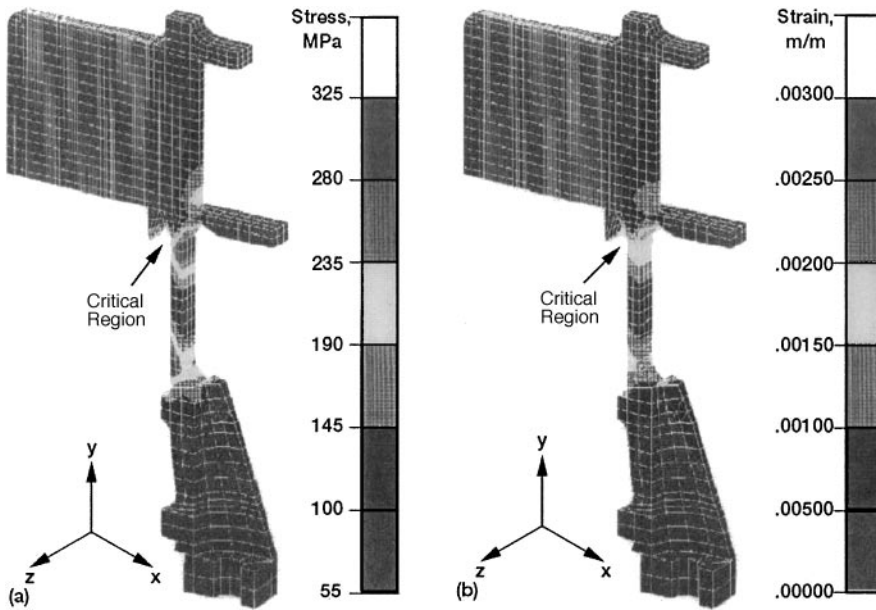
Figure 13. *Von Mises stress and equivalent mechanical strain predicted by Freed's viscoplastic model after 11,000 hours (*a*) Von Mises stress; (*b*) equivalent mechanical strain.*

be shown that there are enough factors of safety in the design to allow for the heater head to meet its design life goals.

The design life of the starfish heater head was 60,000 hours of continuous operation at 775°C. Ideally, to conduct a life approximation analysis for this type of application, 30,000–60,000-hr creep data for Udimet 720 LI is required. This type of data did not exist for Udimet 720 LI. In fact, there were very few materials that have creep data lasting that long. A good life approximation was made based on the data that was generated from this study. By making the assumption that the calculated steady-state creep rates remain constant over the period of interest and the heater head operation is constant (i.e., does not experience
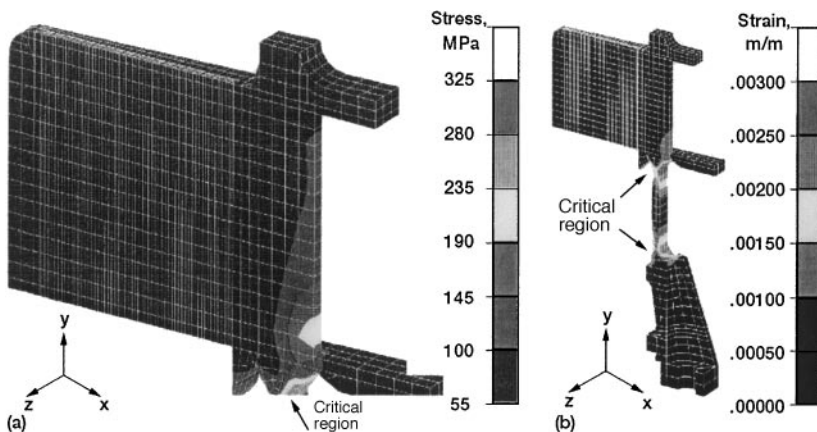

Figure 14. *Von Mises stress and equivalent mechanical strain predicted by Freed's viscoplastic model after 1,001 hours (*a*) Von Mises stress; (*b*) equivalent mechanical strain.*

Figure 15. *Von Mises stress and equivalent mechanical strain predicted by Freed's viscoplastic model after 10,001 hours (*a*) Von Mises stress; (*b*) equivalent mechanical strain.*
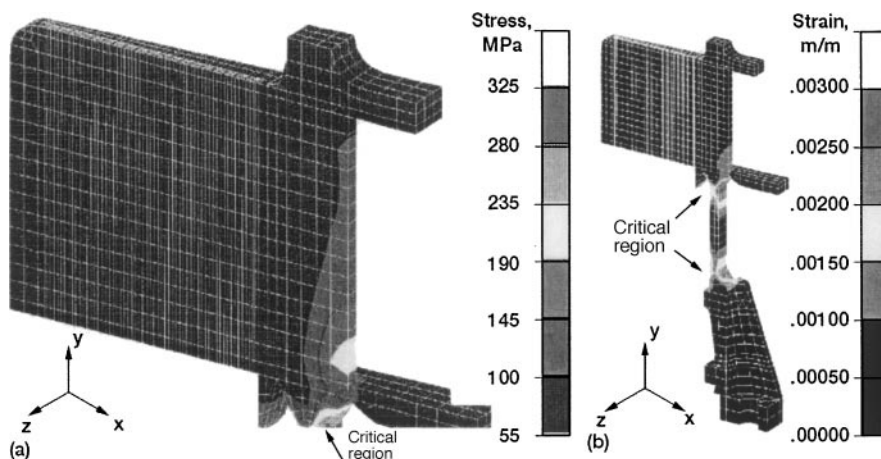
any on-off cycles), a preliminary life approximation was made based on the data presented in Figure 9. For approximately 235 MPa, the calculated maximum heater head stress located at the fin tip, the steady-state creep rate was approximately 4.5×10^{-6} percent/hr. By using a maximum creep strain limit (ASME code case N-47) of 1% as a failure criterion, it would take approximately 222,000 hours to reach that creep strain level. This time to 1% creep strain far exceeded the required design life of 60,000 hours. Conversely, by using the same creep rate for 60,000 hours, the Udimet 720 LI would have accumulated only 0.27% creep strain, which was below the failure criterion of 1%.

In the location of the gas passages, the maximum heater head stresses were approximately 140 MPa. By using a stress value of 280 MPa or a stress value two times larger than the calculated stress from Figure 9, a steady-state creep rate of 2×10^{-5}%/hr was obtained. This creep rate provided a heater head life of 50,000 hours. Note that this life level was still within the acceptable design limits even though it was less than the 60,000-hours design goal because the stress level that was used is double the actual calculated stress for this location.

Therefore, with such large margins of safety (or conservativeness), it is believed that the heater head is more than likely to meet the design life goals of 60,000 hours even with a decrease in life caused by a sodium interaction with the Udimet 720 LI.

CONCLUSIONS

Low-cycle fatigue and creep experiments on a cast-wrought nickel-base superalloy, Udimet 720 LI, and combined finite element viscoplastic analyses for the Stirling starfish heater head were conducted. All testing was performed at temperatures of 625 to 820°C in air. This work was initiated to generate a unique consistent database in support of a life prediction modeling effort aimed at characterizing Freed's viscoplastic model and verifying the key damage mechanisms.

The test program was successfully completed and a fatigue database was generated for this material for a range of temperature variations. The characterization of Freed's viscoplastic model was successfully implemented and applied to a Stirling engine heater head. The data obtained through the viscoplastic analysis coincided well with the experimental results. Running the analysis to cover a 10,000-hours period showed that the heater head is

very likely to last the design lifetime of 60,000 hours since the stresses relaxed as expected toward the end of the loading cycle. The location of extensive deformation in the component depended on the duration of the loading cycle, thereby implying that the failure of the component also depended on the duration of the loading cycle. Furthermore, the results showed that structural analysis by a viscoplastic model that incorporates two internal state variables was capable of qualitatively predicting the experimentally observed behavior of the material. Based on the preliminary life assessment, the heater head met its 60,000-hours design goals. Factors of safety in the thin-walled gas passages were within acceptable limits (a factor of 2 in stress), and therefore liquid sodium attack in this location should not be a concern.

REFERENCES

[1] J. E. Dudenhoefer and J. M. Winter, Status of NASA's Stirling Space Power Converter Program, NASA TM–104512, 1991.

[2] J. E. Dudenhoefer, J. M. Winter, and D. Alger, Progress Update of NASA's Free-Piston Stirling Space Power Converter Technology Project, NASA TM–105748, 1992.

[3] L. G. Thieme and D. M. Swec, Summary of the NASA Lewis Component Technology Program for Stirling Power Converters, NASA TM–105640, 1992.

[4] M. T. Tong, P. A. Bàrtolotta, G. R. Halford, and A. D. Freed, Stirling Engine-Approach for Long-Term Durability Assessment, Proceedings of the 27th Intersociety Energy Conversion Engineering Conference, vol. 5, pp. 209–214, SAE, Warrendale, Pennsylvania, 1992.

[5] R. W. Swindeman and Y. Asada, High-Temperature Service and Time-Dependent Failure, Presented at the Pressure Vessel and Piping Conference, PVP vol. 262, ASME, New York, 1993.

[6] D. A. Freed, P. K. Walker, and J. M. Verrilli, Extending the Theory of Creep to Viscoplasticity, Proceeding of Constitutive Modeling and Applications for High Temperature Structures, S. J. Chang and R. W. Swindeman (eds.), ASME Pressure Vessel and Piping Conference, Denver, July 25–29, 1993.

[7] MARC General Purpose Finite Element Program, MARC Analysis Research Corp., Palo Alto, California, 1983.

[8] J. R. Ellis and P. A. Bartolotta, Adjustable Induction-Heating Coil, NASA Tech. Brief, N–87–26399, vol. 14, no. 11, p. 50, Nov. 1990.

[9] J. L. Chaboche, Viscoplastic Constitutive Equations for the Description of Cyclic and Anisotropic Behavior of Metals, *Bul. Acad. Pol. Sci, Ser. Sci. Technology*, vol. 94, pp. 39–48, 1977.

[10] A. Miller, An Inelastic Constitutive Model for Monotonic, Cyclic, and Creep Deformation, *J. Engrg. Mater. Techol.*, vol. 98, pp. 97–105, 1976.

[11] A. D. Freed and K. P. Walker, Viscoplastic Model Development With an Eye Toward Characterization, *ASME Trans. J. of Eng. Mater. Technol.*, vol. 117, pp. 8–13, Jan. 1995.

[12] R. L. McKnight, J. H. Laflen, and G. T. Spamer, Turbine Blade Tip Durability Analysis, NASA CR–165268, 1981.

[13] V. Moreno, Combustor Liner Durability Analysis, NASA CR–165250, 1981.

[14] E. Krempl, Cyclic Creep: An Interpretive Literature Survey, Welding Research Council Bulletin, no. 195, pp. 63–123, 1974.

[15] C. Zener and J. H. Hollomon, Effects of Strain Rate Upon Plastic Flow of Steel, *J. Appl. Phys.*, vol. 15, pp. 22–32, 1944.

[16] MSC/PATRAN Graphics and Finite Element Package, Vols. II and I, The MacNeal-Schwendler Corporation, Costa Mesa, California, 1997.

[17] W. M. Kays and M. E. Crawford, *Convective Heat And Mass Transfer*, Second Edition, McGraw-Hill Book Company, 1980.

[18] V. K. Arya, Finite Element Analysis of Structural Components Using Viscoplastic Models With Application to a Cowl Lip Problem, Materials at High Temperatures, vol. 9, no. 4, pp. 201–208, Nov. 1991.

[19] V. K. Arya, K. Hornberger, and H. Stamm, On the Numerical Integration of Viscoplastic Models: High Temperature Materials, KfK–4082, 1986.